Weierstraß-Institut
für Angewandte Analysis und Stochastik
Leibniz-Institut im Forschungsverbund Berlin e. V.

Preprint ISSN 0946 – 8633

Self-heating, bistability, and thermal switching in organic semiconductors

Axel Fischer[1], Paul Pahner[1], Björn Lüssem[1], Karl Leo[1], Reinhard Scholz[1],

Thomas Koprucki [2], Klaus Gärtner[2], Annegret Glitzky[2]

submitted: September 19, 2012

[1] Institut für Angewandte Photophysik (IAPP)
Technische Universität Dresden
George-Bähr-Straße 1
01069 Dresden, Germany
E-Mail: axel.fischer@iapp.de
paul.pahner@iapp.de
bjoern.luessem@iapp.de
karl.leo@iapp.de
reinhard.scholz@iapp.de

[2] Weierstraß-Institut
Mohrenstraße 39
10117 Berlin
Germany
E-Mail: thomas.koprucki@wias-berlin.de
klaus.gaertner@wias-berlin.de
annegret.glitzky@wias-berlin.de

No. 1735
Berlin 2012

2010 *Mathematics Subject Classification.* 82D37, 80A20, 34C55.

2008 *Physics and Astronomy Classification Scheme.* 81.05.Fb, 73.61.Wp, 72.80.Le.

Key words and phrases. Organic semiconductor, C_{60}, Joule self-heating, S-shaped negative differential resistance (SNDR), thermal switching, bistability, hysteresis, Arrhenius-like conductivity law.

The work leading to these results has been received founding from the Deutsche Forschungsgemeinschaft (DFG) within the collaborative research center SFB 787 Semiconductor Nanophotonics (Th. Koprucki), DFG Research Center MATHEON under project D22 (A. Glitzky), and by the European Communitys Seventh Framework Programme under Grant Agreement No. FP7-267995 — NUDEV— (A. Fischer).

Edited by
Weierstraß-Institut für Angewandte Analysis und Stochastik (WIAS)
Leibniz-Institut im Forschungsverbund Berlin e. V.
Mohrenstraße 39
10117 Berlin
Germany

Fax: +49 30 20372-303
E-Mail: preprint@wias-berlin.de
World Wide Web: http://www.wias-berlin.de/

Abstract. We demonstrate electric bistability induced by the positive feedback of self-heating onto the thermally activated conductivity in a two-terminal device based on the organic semiconductor C_{60}. The central undoped layer with a thickness of 200 nm is embedded between thinner n-doped layers adjacent to the contacts minimizing injection barriers. The observed current-voltage characteristics follow the general theory for thermistors described by an Arrhenius-like conductivity law. Our findings including hysteresis phenomena are of general relevance for the entire material class since most organic semiconductors can be described by a thermally activated conductivity.

Temperature-activated processes are omnipresent, e.g. in chemical and biochemical reactions or charge carrier and exciton transport and trapping dynamics in solids. Current flow through a solid generates Joule heat, resulting in an increased temperature with respect to the environment. In materials with a positive temperature coefficient of the conductivity, a rising temperature induces a current enhancement and an increased power dissipation, so that this electrothermal feedback loop favors a self-heating mechanism limited by heat losses towards the surroundings. This self-heating phenomenon was first studied in the investigation of the electrical breakdown of dielectrics induced by a thermal runaway [1, 2], where above a certain threshold voltage the cooling of the device is no more sufficient to keep the system in a stationary state. Furthermore, self-heating induces many thermal runaway and switching phenomena, including chemical reactions [3], thermistors [4, 5], semiconductors [6, 7], and transport through thin films [8, 9, 10]. Here, we show that thermal runaway phenomena are also crucial for the materials class of organic semiconductors, which is currently intensively investigated due to its interesting physics and promising device applications.

For materials with Arrhenius-like conductivity laws, self-heating phenomena only occur for activation energies $E_a > 4\,k_{\mathrm{B}}T_a$, where k_{B} denotes Boltzmann's constant and T_a the ambient temperature, see [11]. A characteristic feature of organic semiconductors is a temperature activated conductivity arising from hopping transport. Typically, the mobility μ of carriers follows a law $\mu \propto \exp(-\mathrm{const}/T^n)$, where n varies between 1 and 2 depending on the charge carrier concentration [12]. In disordered organic semiconductors, the density of states can be described by a Gaussian proportional to $\exp[-\frac{1}{2}(E-E_0)^2/\sigma^2]$. The width σ is usually in the range between $2\,k_{\mathrm{B}}T_a$ and $6\,k_{\mathrm{B}}T_a$, resulting in activation energies of $4\,k_{\mathrm{B}}T_a$ to $36\,k_{\mathrm{B}}T_a$ [13]. At interfaces between the organic materials and metallic contacts, injection barriers up to several tenths of an eV result either in thermionic injection or in the formation of a Schottky barrier. It is common practice to reduce these injection barriers by doping the layers adjacent to the contacts, resulting in Arrhenius-like conductivity-temperature laws [14].

Surprisingly, even though activation energies above $4\,k_{\mathrm{B}}T_a$ are quite common in organic semiconductors, the positive feedback between Joule heating and a subsequent thermal runaway has not been observed yet. The crucial role of Joule heating on the device performance has already been considered for fast rectifying diodes [15] and for organic light-emitting diodes (OLEDs) [16]. However, in these devices a thermal runaway was probably inhibited by a series resistance within the circuit, arising e.g. from an indium-tin-oxide electrode.

Here, we demonstrate electrothermal bistability for vertical crossbar structures based on the organic semiconductor C_{60}. It is shown that an abrupt turnover from a low conductive to a highly conductive state follows in a natural way from the current-voltage characteristics predicted by theory.

First, we summarize the theory of self-heating for a thermally activated conductivity and suppose in the following that the isothermal current-voltage relation for the circuit is given by a power law

$$I_{\mathrm{iso}}(U,T) = I_{\mathrm{ref}} \left(\frac{U}{U_{\mathrm{ref}}}\right)^{\alpha} F(T) \tag{1}$$

with a positive exponent α and a temperature-dependent conductivity factor $F(T)$ resulting from an Arrhenius law

$$F(T) = \exp\left[-\frac{E_a}{k_{\mathrm{B}}}\left(\frac{1}{T} - \frac{1}{T_a}\right)\right]. \tag{2}$$

The quantities U_{ref}, I_{ref}, and $P_{\mathrm{ref}} = U_{\mathrm{ref}} I_{\mathrm{ref}}$ denote reference values for voltage, current and power, respectively. The homogeneous steady states of the device are given by equilibria of the global heat balance equation expressing that the dissipated Joule power $\dot{Q}_2 = IU$ equals the heat loss $\dot{Q}_1 = \frac{1}{\Theta_{\mathrm{th}}}(T - T_a)$ to the surrounding described by the thermal resistance Θ_{th},

$$\frac{1}{\Theta_{\mathrm{th}}}(T - T_a) = P_{\mathrm{ref}} \left(\frac{U}{U_{\mathrm{ref}}}\right)^{\alpha+1} F(T). \tag{3}$$

The self-consistent current-voltage characteristic including self-heating parametrized by the temperature $T \geq T_a$ is obtained by combining Eqs. (1) and (3),

$$U(T) = U_{\mathrm{ref}} \left(\frac{T - T_a}{\Theta_{\mathrm{th}} P_{\mathrm{ref}}}\right)^{\frac{1}{\alpha+1}} F(T)^{-\frac{1}{\alpha+1}}, \tag{4}$$

$$I(T) = I_{\mathrm{ref}} \left(\frac{T - T_a}{\Theta_{\mathrm{th}} P_{\mathrm{ref}}}\right)^{\frac{\alpha}{\alpha+1}} F(T)^{\frac{1}{\alpha+1}}. \tag{5}$$

Different points on the self-consistent current-voltage characteristic correspond to different values of the temperature rise $T - T_a$. The differential resistance of this S-shaped curve has the form

$$\frac{dU}{dI} = \frac{1 - (T - T_a)\frac{d}{dT}\ln F(T)}{\alpha + (T - T_a)\frac{d}{dT}\ln F(T)} \, \frac{U}{I}. \tag{6}$$

For $T - (\frac{d}{dT}\ln F(T))^{-1} > T_a$ a region of negative differential resistance (NDR) is obtained. In the Arrhenius type temperature dependence Eq. (2) a NDR region only appears for activation energies $E_a > 4\,k_{\mathrm{B}}T_a$. This can be seen in Fig. 1 where the self-consistent IV curve of such an intrinsic device is shown for an isothermal Ohmic current-voltage relation ($\alpha = 1$, $U_{\mathrm{ref}}/I_{\mathrm{ref}} = 2000\,\Omega$) The turnover points of the S-shaped IV curve are characterized by the condition $\frac{dU}{dI} = 0$. For $E_a > 4\,k_{\mathrm{B}}T_a$, irrespective of the exponent α in Eq. (1), the temperature increase $\Delta T_{1,2} = T_{1,2} - T_a$ at the two turnover points becomes

$$\frac{\Delta T_{1,2}}{T_a} = \frac{E_a}{2k_{\mathrm{B}}T_a}\left(1 \mp \sqrt{1 - \frac{4k_{\mathrm{B}}T_a}{E_a}}\right) - 1. \tag{7}$$

The temperature rises at the turnover points depend only on the normalized activation energy, $E_a/(k_{\mathrm{B}}T_a)$. Along the S-shaped current-voltage characteristics, two stable branches exist: a highly conducting 'ON' state and a low conducting 'OFF' state, whereas the intermediate NDR region is unstable, see Fig. 1. This bistable behavior of the IV characteristic is related to thermal switching at the turnover points with $dI/dU \to \infty$, involving a hysteresis loop [17, Ch. 6.2], where

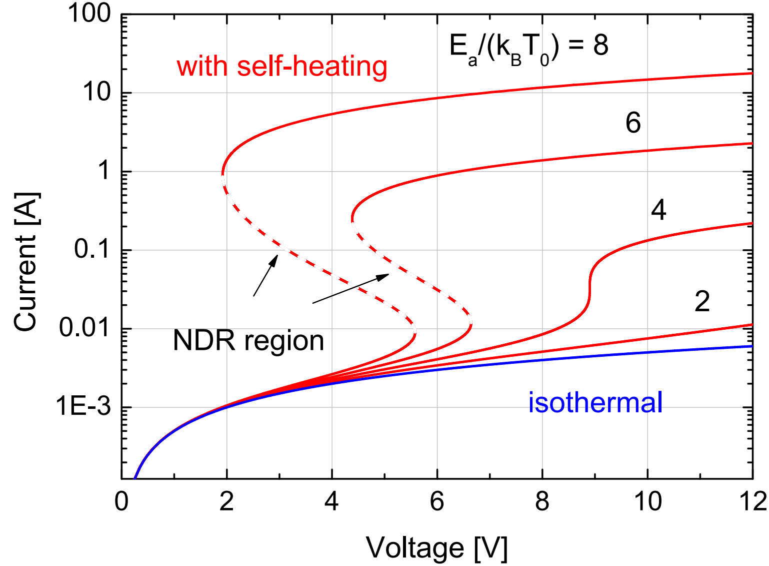

FIGURE 1. Self-consistent current-voltage characteristics including self-heating (red), revealing that thermal switching can only occur above the critical value of the activation energy, $E_a > 4\,k_{\mathrm{B}}T_a$. Unstable NDR regions are indicated by dashed lines. Thermal resistance $\Theta_{\mathrm{th}} = 1000\,\mathrm{K/W}$. Blue: linear isothermal current-voltage relation at ambient temperature T_a.

the switching between the low conductivity OFF and the high conductivity ON branches occurs.

The IV characteristics of the intrinsic device showing the pure S-shaped NDR (S-NDR) behavior described by Eqs. (4) and (5) together with a load resistance R_{L} in series can again be parameterized by an increased temperature $T \geq T_a$. The resulting characteristic $(U_{\mathrm{tot}}(T), I(T))$ involves a modified total voltage along the load line $U_{\mathrm{tot}}(T) = U(T) + R_{\mathrm{L}}I(T)$, where $U(T)$ and $I(T)$ are defined in Eqs. (4) and (5), respectively. Turnover points are characterized by $\frac{dU}{dI} + R_{\mathrm{L}} = 0$, corresponding to a tangency condition for the intersection points between the load line and the IV characteristic of the S-NDR element itself [17, 6, Ch. 6.2]. For sufficiently small load resistance, namely for $-\min \frac{dU}{dI} > R_{\mathrm{L}}$, the hysteresis effect is preserved, so that thermal switching between the ON and OFF states remains possible. The impact of a load resistance on the IV characteristic of the circuit is shown in Fig. 2 for a device with linear isothermal IV relation ($\alpha = 1$, $U_{\mathrm{ref}}/I_{\mathrm{ref}} = 2000\,\Omega$).

By an appropriate choice of the load resistance, it may be possible to reduce the dissipated power in the ON state to a value that does not destroy the device by thermal runaway, but still preserving thermal switching. Further increase of the load resistance suppresses thermal switching ($R_{\mathrm{L}} > 55\,\Omega$), but leads to a stabilization of the NDR region present in the intrinsic device [17, Ch. 6.2]. For large voltages, the behavior is asymptotically dominated by the load resistance, see Fig. 2.

A suitable test structure requires an organic material with a sufficiently large conductivity, an activation energy $E_a > 4\,k_{\mathrm{B}}T_a$, thermal stability up to rather high temperatures, and negligible influence of injection barriers. Moreover, the thermal resistance Θ_{th} must lead to a substantial increase of the device temperature at moderate voltages.

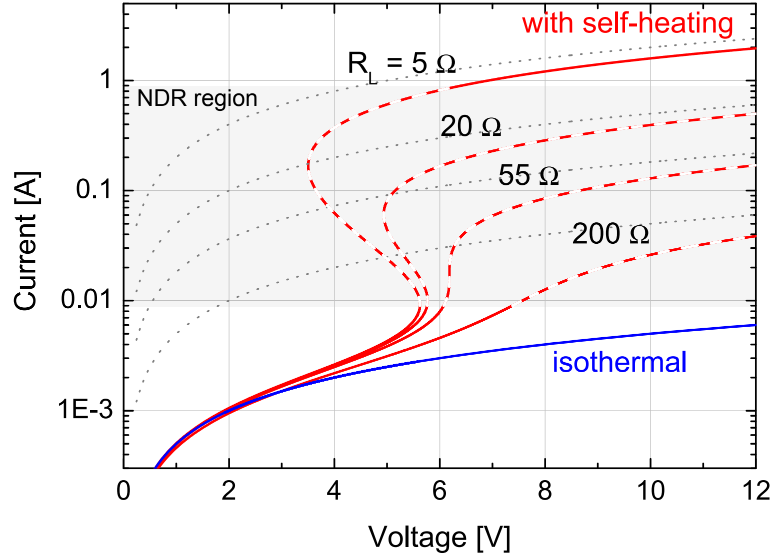

FIGURE 2. Current-voltage characteristics of an electrical circuit consisting of a device including self-heating, together with a load resistance R_{L} in series (red), for $E_a = 8\,k_{\mathrm{B}}T_a$, a thermal resistance $\Theta_{\mathrm{th}} = 1000\,\mathrm{K/W}$, and different values of the load. The dashed parts indicate the NDR region of the intrinsic device as shown in Fig. 1. Blue: linear isothermal current-voltage relation at constant temperature T_a, black dotted: load resistance only.

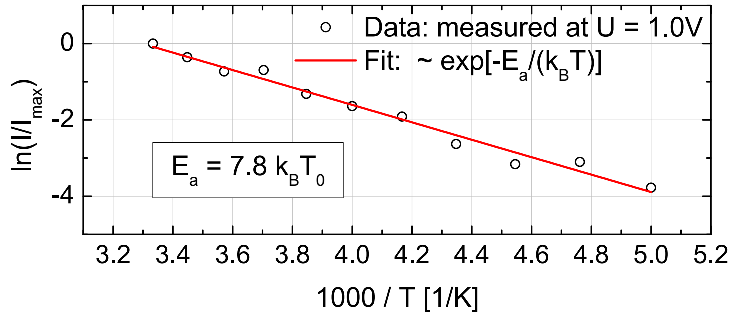

FIGURE 3. Measurement of the current at $U = 1.0\,\mathrm{V}$ over temperature, revealing an activation energy of $E_a = 7.8\,k_{\mathrm{B}}T_0$.

All these requirements are perfectly met by nin-C_{60} crossbar structures grown on glass substrates, employing 20 nm thick n-doped C_{60} (n-C_{60}) layers adjacent to the metallic contacts, an intrinsic layer (i-C_{60}) with a thickness of 200 nm in between, and a relatively small active area of about $0.06\,\mathrm{mm}^2$. Details of the sample geometry have been published elsewhere together with the measured and simulated temperature distribution in the device [18].

From conductivity measurements in the temperature range from 200 K to 300 K, we have obtained an activation energy of $7.8\,k_{\mathrm{B}}T_0$, $T_0 = 293\,\mathrm{K}$, sufficiently large to allow for thermal switching, compare Fig. 3. In these measurements, the voltage is kept fixed at a rather low value of 1 V in order to avoid self-heating. Please note that the activation energy is not an intrinsic feature of the C_{60} material, but rather depends on the entire device geometry.

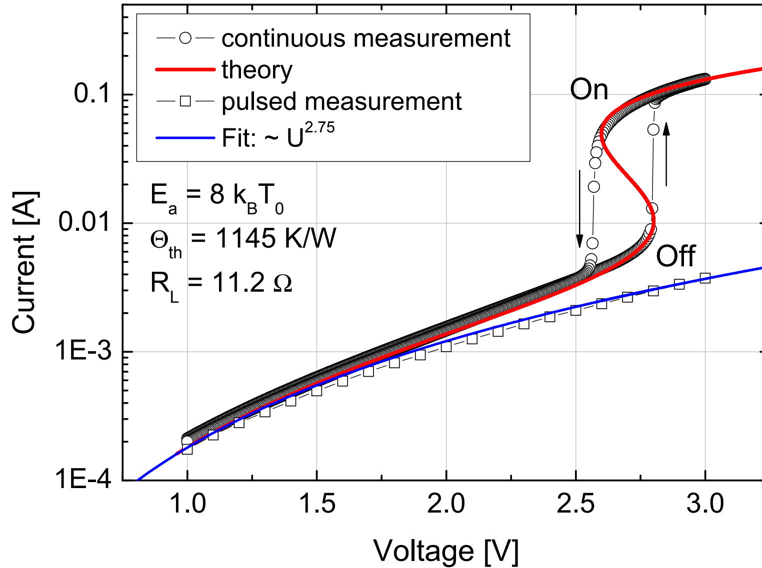

FIGURE 4. Thermal switching measured during a voltage sweep upwards and downwards. For comparison, an isothermal current voltage characteristic is measured by applying short voltage pulses. The sample is cooled to $T_a = -52°\text{C}$ (221 K).

Since thermal switching is accompanied by a large increase of the sample temperature, it was found convenient to reduce the ambient temperature to a value of $T_a = 221$ K by a Peltier cryostat. The resistance of electrodes and measurement setup is about $7\,\Omega$ [18] and is increased by an additional series resistance of $5\,\Omega$.

The current-voltage characteristics in Fig. 4 are measured in a voltage sweep from 1 V to 3 V and back, with voltage steps of 5 mV held for time intervals of 0.15 s using a Keithley SMU 2400. At a voltage of 2.80 V, the circuit switches from the low conductivity OFF state to the high conductivity ON state. As long as we apply sufficiently large voltages, the system stays on the upper branch, but at 2.57 V it switches back to the OFF state, with a pronounced hysteresis between the two switching voltages. The thermal character of the switching becomes obvious when comparing to a measurement with short voltage pulses (Keithley 2635A, pulse width: 200 μs, repetition time: 200 ms). In this measurement, the curve can simply be described by a power law with an exponent $\alpha = 2.75$, $U_{\text{ref}} = 23\,\text{V}$ and $I_{\text{ref}} = 1\,\text{A}$ in Eq. (1), without any signature of an increase in sample temperature.

The theoretical approach outlined above can be used to assign the key parameters of our device. Applying Eqs. (4) and (5) together with a load resistance, we obtain the best agreement between measured and calculated current-voltage characteristics when assuming an activation energy of $E_a = 8\,k_{\text{B}}T_0 = 10.6\,k_{\text{B}}T_a$, in good agreement with the value obtained for a fixed value of $U = 1$ V, a load resistance of $R_{\text{L}} = 11.2\,\Omega$, and a thermal resistance of $\Theta_{\text{th}} = 1145$ K/W, see Fig. 4. The thermal resistance is in the same range as a value of about 1000 K/W obtained by simulations of the heat flow [18].

Our fitting procedure demonstrates that the bistability is a natural consequence of the thermally activated conductivity in the organic electronic circuit. Residual deviations between theory and measurement along ON state at a voltage about 2.6 V maybe due to the simplifying assumption of homogeneous steady-states. After switching back to the OFF state, the voltage sweep downwards reproduces the

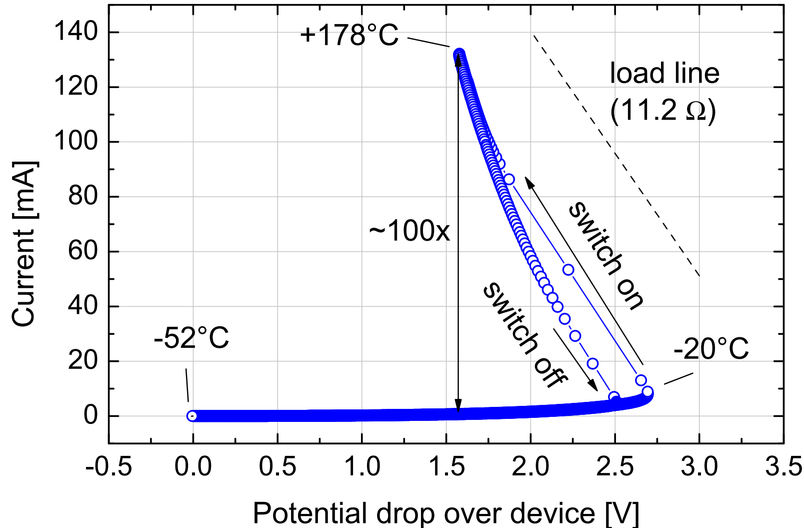

FIGURE 5. Current-voltage characteristics as a function of the potential drop over the organic S-NDR element recovered by subtracting the voltage drop over the load resistance R_{L} showing the switching along the load line. The dashed line is a guide to the eye for a load line corresponding to $R_{\mathrm{L}} = 11.2\,\Omega$. The highest temperature achieved is about 178°C, or 230 K above the ambient temperature in the Peltier cooler.

previous sweep upwards, indicating that the device has not been damaged by passing through the entire hysteresis loop. Possible influences of a phase change of the organic material, e.g. a transition from a simple cubic to a face-centred cubic lattice structure at 251 K, compare [19], can be excluded because we cannot observe any deviation of the conductivity from Eqs. (4) and (5). Changes of charge carrier concentration due to impact ionization at high electric fields can be neglected since they cannot contribute significantly at voltages below 3 V [20].

Consequently, the conductivity switching can be completely explained by purely thermal effects, revealing that nin-C_{60} devices constitute an interesting model system for further studies of thermally induced bistability.

The S-shaped IV curve of thermistors possesses an NDR region induced by self-heating. We are not able to measure the IV characteristic of the S-NDR element directly since a certain series resistance is already included within the device and measurement setup. Typically, such measurements are realized by a high load resistor which stabilizes the NDR region and prevents thermal switching. To recover the pure IV curve of the organic S-NDR element we use the load line to subtract the voltage drop over the load resistance $R_{\mathrm{L}} = 11.2\,\Omega$ as determined by the fit to theory before. In Fig. 5, the measured current is plotted as a function of the recalculated voltage drop over the crossbar structure. While switching into the ON state along the load line, the device exhibits a NDR, resulting in a strong reduction of resistance by a factor of more than 100. By using the analytical expression underlying the fit of the experimental data, we can estimate the temperature at each point on the curve. As the highest temperature, we obtain 178°C, still significantly below values of more than 200°C obtained when stressing similar devices at even higher voltages [18].

In conclusion, for organic semiconductors we have demonstrated thermal switching and a pronounced hysteresis loop as a natural consequence of the bistability induced by a S-shaped IV characteristic. A significant impact of further phenomena like phase changes, device degradation, or electronic effects like field ionization can be excluded, making these easy-to-build C_{60}-crossbar structures an ideal model system for studies of thermal runaway phenomena. Since almost all organic semiconductors show Arrhenius-like conductivity laws, our results have a significant impact on various types of organic devices, including OLEDs, OFETs, and high-power rectifying diodes. Even in cases where thermal switching is inhibited by a large series resistance, self-heating can lead to a negative differential resistance, so that all organic devices with sufficiently large activation energies have to be understood as thermistors. This implies that the positive feedback between temperature and conductivity has to be considered in device simulations together with an analysis of the heat conduction away from the organic circuit. As will be discussed elsewhere in more detail, we observed S-NDR in OLED devices, enhancing the spatial inhomogeneity of power dissipation and light emission in OLED lighting panels [21]. Moreover, self-heating can promote current filaments [22, 11] or other spatial inhomogeneities [17], so that three-dimensional simulations of transport through organic materials with negative differential resistance will become mandatory for a deeper understanding of charge and heat transport.

Acknowledgement

The work leading to these results has received funding from the DFG (Deutsche Forschungsgemeinschaft) within the collaborative research center CRC 787 "Semiconductor Nanophotonics" (Th. Koprucki), the DFG Research Center MATHEON under project D22 (A. Glitzky), and by the European Community's Seventh Framework Programme under Grant Agreement No. FP7-267995 (NUDEV) (A. Fischer).

References

[1] Karl Willy Wagner. The Physical Nature of the Electrical Breakdown of Solid Dielectrics. *Transactions of the American Institute of Electrical Engineers*, 41:288 – 299, 1922.

[2] Lydia Inge, N. Semenoff, and Alexander Walther. Über den Durchschlag fester Isolatoren. *Zeitschrift für Physik A Hadrons and Nuclei*, 32:273–286, 1925.

[3] N. Semenoff. Zur Theorie des Verbrennungsprozesses. *Zeitschrift für Physik A Hadrons and Nuclei*, 48:571–582, 1928.

[4] J. A. Becker, C.B. Green, and G. L. Pearson. Properties and Uses of Thermistors — Thermally Sensitive Resistors. *Transactions of the American Institute of Electrical Engineers*, 65:711 – 725, 1946.

[5] R E Burgess. The Turnover Phenomenon in Thermistors and in Point-Contact Germanium Rectifiers. *Proceedings of the Physical Society. Section B*, 68(11):908–917, 1955.

[6] Corneliu Popescu. Selfheating and thermal runaway phenomena in semiconductor devices. *Solid-State Electronics*, 13(4):441 – 450, 1970.

[7] N. Croitoru and C. Popescu. Thermal Mechanism of the Switching Phenomenon. *physica status solidi (a)*, 3(4):1047–1055, 1970.

[8] N. Klein. Switching and breakdown in films. *Thin Solid Films*, 7:149 – 177, 1971.

[9] C.N. Berglund and N. Klein. Thermal effects on switching of solids from an insulating to a conductive state. *Proceedings of the IEEE*, 59:1099 – 1110, 1971.

[10] W. Haubenreisser, W. Löser, C. Mattheck, K.-H. Möckel, and E. Steinbeiss. Co_3O_4 as a model substance for thermistor effect switching in coplanar thin film devices. *physica status solidi (a)*, 22(2):427–434, 1974.

[11] M.P. Shaw, V.V. Mitin, E. Schöll, and H.L. Grubin. *The Physics of Instabilities in Solid State Electron Devices*. Plenum Press, New York, 1992.

[12] Heinz Bässler and Anna Köhler. Charge Transport in Organic Semiconductors. In Robert M. Metzger, editor, *Unimolecular and Supramolecular Electronics I*, volume 312 of *Topics in Current Chemistry*, pages 1–65. Springer Berlin / Heidelberg, 2012.

[13] W. F. Pasveer, J. Cottaar, C. Tanase, R. Coehoorn, P. A. Bobbert, P. W. M. Blom, D. M. de Leeuw, and M. A. J. Michels. Unified Description of Charge-Carrier Mobilities in Disordered Semiconducting Polymers. *Phys. Rev. Lett.*, 94(20):206601, 2005.

[14] K. Walzer, B. Maennig, M. Pfeiffer, and K. Leo. Highly Efficient Organic Devices Based on Electrically Doped Transport Layers. *Chem. Rev.*, 107(4):1233–1271, 2007.

[15] Soeren Steudel, Kris Myny, Vladimir Arkhipov, Carsten Deibel, Stijn De Vusser, Jan Genoe, and Paul Heremans. 50 MHz rectifier based on an organic diode. *Nat. Mater.*, 4(8):597–600, 2005.

[16] Jongwoon Park, Jongho Lee, and Yong-Young Noh. Optical and thermal properties of large-area OLED lightings with metallic grids. *Org. Electron.*, 13(1):184–194, 2012.

[17] E. Schöll. *Nonequilibrium Phase Transitions in Semiconductors*. Springer, Berlin Heidelberg, 1987.

[18] Axel Fischer, Paul Pahner, Björn Lüssem, Karl Leo, Reinhard Scholz, Thomas Koprucki, Jürgen Fuhrmann, Klaus Gärtner, and Annegret Glitzky. Self-heating effects in organic semiconductor crossbar structures with small active area. *Org. Electron.*, 13(11):2461–2468, 2012.

[19] He Peimo, Xu Yabo, Zhang Xuejia, Zhen Xinbin, and Li Wenzhou. Electrical conductivity studies of a pure C_{60} single crystal. *Journal of Physics: Condensed Matter*, 5(37):7013–7016, 1993.

[20] G.K. Wachutka. Analytical model for the destruction mechanism of GTO-like devices by avalanche injection. *Electron Devices, IEEE Transactions on*, 38(6):1516–1523, 1991.

[21] Axel Fischer, Reinhard Scholz, Björn Lüssem, Karl Leo, Thomas Koprucki, Klaus Gärtner, and Annegret Glitzky. Unpublished results.

[22] J. J. M. van der Holst, M. A. Uijttewaal, B. Ramachandhran, R. Coehoorn, P. A. Bobbert, G. A. de Wijs, and R. A. de Groot. Modeling and analysis of the three-dimensional current density in sandwich-type single-carrier devices of disordered organic semiconductors. *Phys. Rev. B*, 79(8):085203, 2009.